



Max Planck WinDarts: High-Resolution Atmospheric Boundary Layer Measurements with the Max Planck CloudKite platform and Ground Weather Station – A Data Overview

Venecia Chávez-Medina¹, Hossein Khodamoradi¹, Oliver Schlenczek¹, Freja Nordsiek^{1,2}, Claudia E. Brunner¹, Eberhard Bodenschatz^{1,3,4}, and Gholamhossein Bagheri¹

¹Max Planck Institute for Dynamics and Self-Organization (MPI-DS), Am Faßberg 17, 37077 Göttingen, Germany

²Gesellschaft für wissenschaftliche Datenverarbeitung mbH Göttingen (GWDG), Burckhardtweg 4, 37077 Göttingen, Germany

³Institute for Dynamics of Complex Systems, Georg August University of Göttingen, Friedrich-Hund-Platz 1, 37077 Göttingen, Germany

⁴Laboratory of Atomic and Solid State Physics and Sibley School of Mechanical and Aerospace Engineering, Cornell University, 130 Upton Hall, Ithaca NY 14853, USA

Correspondence: Gholamhossein Bagheri (gholamhossein.bagheri@ds.mpg.de)

Abstract.

This paper presents the data set collected during the Pallas Cloud Experiment (PaCE) campaign, conducted at Pallas, Finland, between September 15 and September 28, 2022. The data set includes measurements of turbulence in the atmospheric boundary layer in both cloudy and cloud-free conditions, collected using the Max Planck CloudKite (MPCK) platform, the WinDarts, and a ground weather station for near surface data. The airborne observations span altitudes from the surface up to 1510 m above ground level, with flight durations ranging from 1 hour to nearly 6 hours, while the ground weather station provides continuous measurements throughout the entire campaign. This data set provides high-resolution meteorological measurements to analyse boundary layer dynamics under different atmospheric conditions encountered during PaCE campaign. This paper describes the data collection process, the structure of the data set, and guidelines for users.

10 1 Introduction

The atmospheric boundary layer (ABL) is the lower fraction of the atmosphere in direct contact with the Earth's surface. Its depth and structure vary depending on weather conditions, latitude, terrain, and time of day, typically ranging from a few hundred meters to a couple of kilometres. Understanding the physical processes that govern its dynamics—such as turbulence, wind shear, convective structures, and entrainment—is crucial for many practical applications, including, for example, weather prediction and aviation.

In-situ velocity, temperature, and relative humidity measurements are essential for a thorough understanding of turbulence in the ABL, as they capture real-world interactions. In particular, temperature and vertical velocity play a key role in understanding air mass behaviour, turbulence, and vertical motion, which drive atmospheric dynamics. Time series data from different regions of the ABL provide valuable insights into these processes, improving our understanding of boundary layer properties such as



20 depth, stability, and surface interactions. Moreover, such measurements are needed for refining numerical weather models and climate simulations by better characterizing key processes like heat exchange, vertical mixing, boundary layer evolution, and convection.

Obtaining in-situ measurements of the ABL remains a significant challenge. The three most widely used techniques, namely tower-based, instrumented aircraft observations, and radiosondes, each have strengths and limitations. Tower-based measurements offer exceptional spatio-temporal resolution but are limited in altitude. Instrumented aircraft can probe the upper ABL but struggle to access lower levels, and their high relative speed reduces spatial resolution. Radiosondes provide flexibility in launch locations and vertical range but are advected by atmospheric currents, preventing them from maintaining a steady altitude, which is needed to gather enough statistics at a given height.

To address these challenges, the Max Planck WinDarts, developed by the CloudKite team, provide a novel solution. They are deployed as part of the Max Planck CloudKite (MPCK) platform, which integrates a tethered balloon-kite hybrid (Helikite) along with complementary ground-based and airborne instruments. They bridge the gap between tower-based and instrumented aircraft measurements by enabling controlled profiling of the entire ABL under most atmospheric conditions. These instruments are purpose-built for profiling and characterising the turbulent dynamics of the ABL, offering cutting-edge, in-situ measurements of critical meteorological quantities, including temperature, humidity, wind speed, and pressure. Unlike radiosondes, the flight strategy of the WinDarts can be actively controlled, allowing for targeted observations and improved vertical profiling of the ABL.

To complement the measurements obtained with the WinDarts, a ground weather station also recorded continuous meteorological quantities. These data serve as a baseline for assessing near-surface conditions and evaluating potential gradients between the surface and the altitude ranges sampled by the WinDarts. All together, the data set provides high-resolution measurements of meteorological variables, supporting researchers in studying the atmospheric boundary layer and enabling the characterization of vertical profiles and fluxes across the surface layer, mixed layer, and entrainment zone.

The manuscript focuses on data description and not on scientific analysis, it begins with a brief introduction to the Pallas Cloud Experiment (PaCE) campaign, conducted in Pallas, Finland, in 2022. We present an overview of the campaign and its geographic location. Following, we introduce the Max Planck WinDarts, the ground weather station, and the methodology used during the scientific flights conducted by the CloudKite team. Later, we present a detailed account of the data collected, focusing on raw and post-processed data sets. Finally, we present the file structure and give some notes on data availability, usage notes and intended end users.

This study is part of a special issue on the Pallas Cloud Experiment (PaCE), which brought together multiple observational platforms to investigate ABL processes in a sub-Arctic environment. The data set presented here complements other measurements from the campaign, including remote sensing, UAV observations, and cloud microphysics. For a comprehensive overview of the campaign, including its objectives, instrumentation, and experimental setup, readers are referred to Brus et al. (2025). Another set of atmospheric in-situ data measured with the Advanced Max Planck CloudKite Instrument (MPCK⁺) is published in Schlenczek et al. (2025) within the same special issue.



2 Overview of PaCE campaign

55 The Pallas Cloud Experiment (PaCE) was a field campaign mainly dedicated to conduct semi long-term measurements and characterise aerosols and clouds in vertical column at high resolution at the Pallas-Sodankylä Global Atmosphere Watch (GAW) Sammaltunturi station, operated by the Finnish Meteorological Institute (FMI) in northern Finland's Lapland region (Douglgeris et al., 2022; Brus et al., 2025; Gratzl et al., 2025).

This initiative involved collaboration among various European scientific institutions, each deploying multiple mobile plat-
60 forms to gather data on atmospheric properties (Brus et al., 2025). The campaign ran from September 15 to December 15, 2022, with an intensive period of measurement from September 15 to October 15, employing diverse methods to collect broad data sets. The Max Planck Institute for Dynamics and Self-Organization (MPI-DS), represented by the CloudKite team deploying the MPCK platform, operated from September 12 to September 29, 2022, during which a wide range of atmospheric conditions and phenomena were documented.

65 Other participating institutions include the Finnish Meteorological Institute, the Swiss Federal Institute of Technology Lausanne, the University of Hertfordshire, the Karlsruhe Institute of Technology, and the Vienna University of Technology.

The measuring site is located at 68.0231° N and 24.1636° E, in Finnish Lapland and the western shoreline of Pallasjärvi Lake, approximately 280 m above mean sea level (MSL), and 162 km north of the Arctic Circle. The site is well-suited for in-situ measurements, as it is located within a designated airspace that spans 7 km on each side and extends to an altitude of 2
70 km. For location details, visit <https://en.ilmatieteenlaitos.fi/pallas-atmosphere-ecosystem-supersite>.

3 Instrumentation and methodology

3.1 The Max Planck CloudKite (MPCK) platform

The MPCK platform is composed of two tethered helikites (an aerostat with a helium-filled balloon and a kite attached to it) that combine helium buoyancy with aerodynamic lift from a kite, enabling stable tethered flights with operational heights of up
75 to 2 km controllable by a winch. In PaCE we used the 250 m³ helikite with a 34 m³ stacked on top of it to provide extra helium wind lift. During the campaign, two WinDarts (see subsection 3.2) and a ground weather station (see subsection 3.3) were deployed with the MPCK platform, as illustrated in figure 2, with additional photographs in figure 3 showing a view from the ground station and figure 1 showing the MPCK platform and the ground weather station. During every flight, two WinDarts were positioned along the tether of the MPCK platform. Two other instruments were deployed as part of the MPCK's payload
80 during some flights: the MPCK⁺ and the FishBox. The MPCK⁺ is developed by researchers at the MPI-DS to gain insights into cloud microphysics and turbulence Stevens et al. (2021) and Schröder (2023). The FishBox, measuring mostly aerosol-related quantities, is developed by scientists from the Finnish Meteorological Institute.

In this configuration of the MPCK platform, the secondary Helikite was stacked above the primary one to stabilise the tether and enhance overall buoyancy and payload capacity. This tandem arrangement allowed for a net payload of approximately
85 ~ 100 kg to be lifted to an altitude of 2 km above ground level. The Helikites used in the MPCK platform were the 250 m³ and

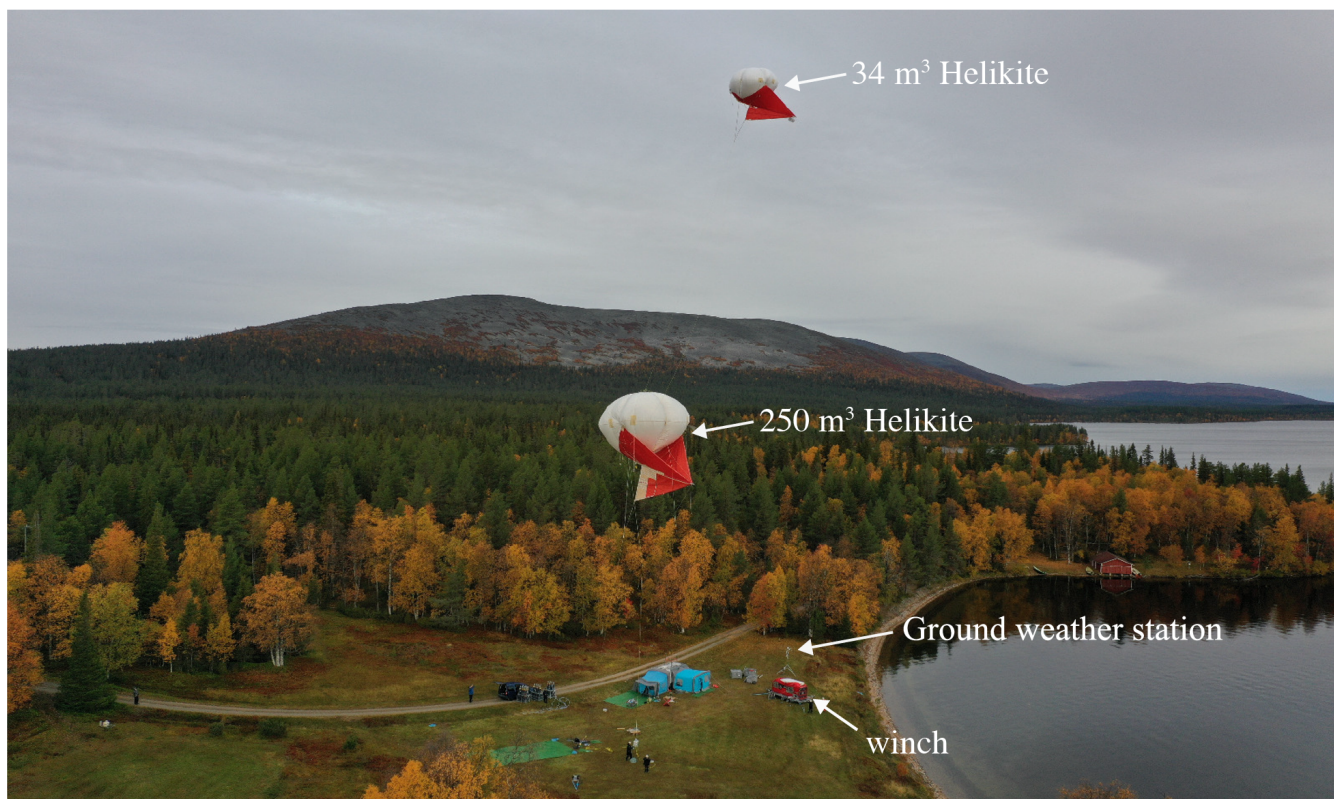


Figure 1. The Max Planck CloudKite (MPCK) platform, and the ground weather station at Pallasjärvi during PaCE 2022.

34 m³ Desert Star models manufactured by Allsopp Helikites. These models were selected for their ability to align with the wind and maintain a stable position within 55° from vertical, ensuring functionality across a broad range of wind conditions. The 250 m³ Desert Star Helikite measures approximately 9.3 m in length and width and stands about 10 m tall. Its keel extends around 9.35 m in length and varies in height between 3.5 - 4.5 m.

90 The winch controls the length of the main tether through a line guidance system, allowing the flight altitude to be adjusted by reeling in or out the main tether, enabling flexible flight-height strategies. The wind lift generated by the Helikite sails was sufficient to reach altitudes at which the WinDarts could sample the mixed layer, the entrainment zone or above it during the campaign.

3.2 WinDarts

95 The Max Planck WinDarts are airborne, purpose-built probes designed as part of the MPCK infrastructure to characterise turbulence in the atmospheric boundary layer (ABL) from ground level up to 2 km above ground level (AGL). Suspended from the tether of the MPCK platform, they provide high spatio-temporal resolution measurements due to their low true air speed

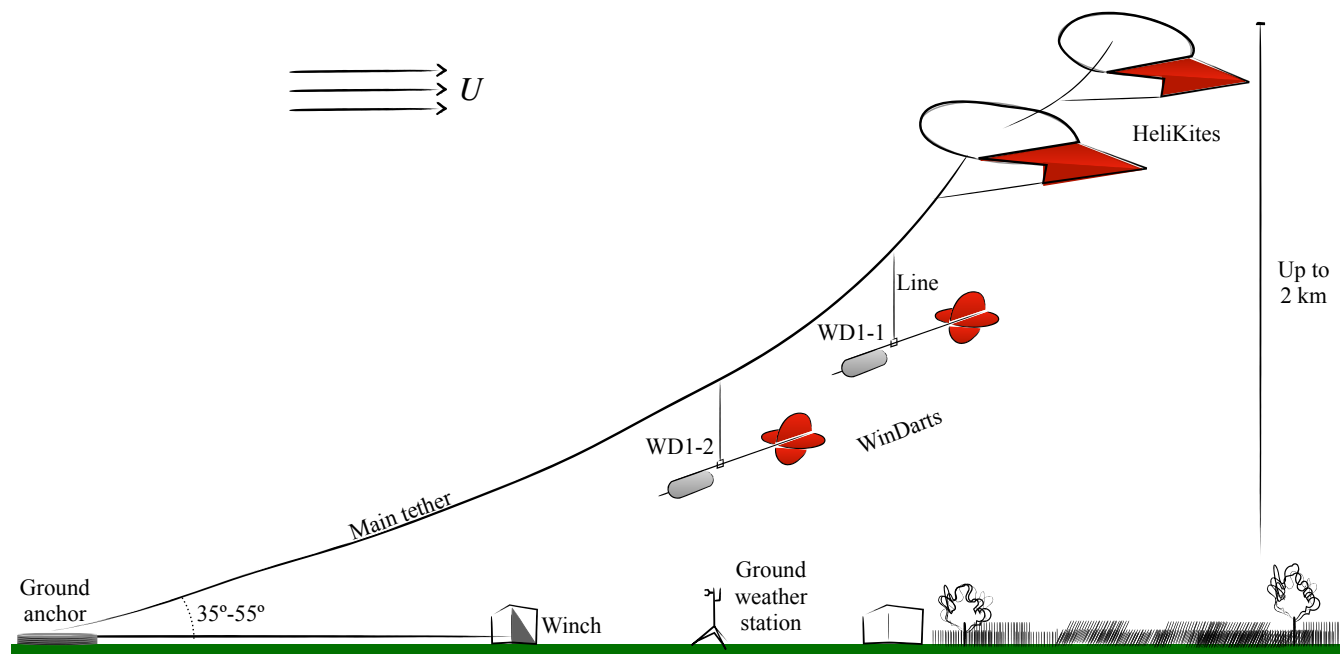


Figure 2. Schematic of the tandem or stacked flight of the two WinDarts and the MPCK platform during the PaCE campaign (not to scale). The winch is anchored to the ground and controls the length of the main tether, which holds the HeliKites (250 m^3 and 34 m^3). The WinDarts are suspended from the main tether via a 5-meter line and a stabiliser. Due to the tail fins, the WinDarts passively align themselves with the mean wind velocity, U .

of the platform combined. Additionally, their ability to align with the mean wind enables extended in-situ observations of key turbulent variables for up to 7 hours of continuous measurement, limited only by their battery capacity.

100 During the campaign, two WinDarts, each weighing approximately 5 kg and measuring 2.5 m in length, were deployed. The WinDarts, labelled WD1-1 and WD1-2, were attached to an independent line and stabiliser hanging from the tether of the MPCK, a configuration that minimises both flow distortion caused by the HeliKite and vibrations transmitted through the tether. This setup ensures the WinDarts remain balanced. Additionally, the WinDarts can passively adjust to the horizontal mean wind direction, and they are light enough that the MPCK platform provides sufficient lift to reach entrainment altitudes.
105 The core electronics are housed in waterproof casings to protect against dust, splashes, and water droplets. Figure 4 presents a CAD rendering of the WinDart.

Each WinDart is equipped with sensors that record time series data for three-dimensional (3D) wind velocity, temperature, absolute pressure, relative humidity, as well as CO_2 , volatile organic compounds (VOC) and particle concentration ($0.3\text{--}40 \text{ }\mu\text{m}$). Each measurement is time-stamped and geographically referenced. Table 1 provides an overview of its measurement



Figure 3. (Left) The aerostats of the MPCK platform (1, 2) lift a WinDart (5), which is connected to a line (4) and stabiliser, both attached to the main tether of the MPCK (3). (Right) The ground weather station with its main components: (1) Metek uSonic3 Class A-MP anemometer, (2) Lufft WS500UMB weather station including pressure, temperature, humidity and 2D wind velocity sensor, (3) Li-Cor LI-7500DS fast trace gas and humidity sensor, (4) Boltek LD-250 lightning detector, and (5) Campbell Scientific CS110 electric field meter.

110 devices, including the measured quantities and acquisition frequencies, and figure 4 indicates the location of each sensor. The design incorporates redundancy for key measurements to enhance data reliability.

3.2.1 Overview of the scientific flights

The first scientific flight with the WinDarts took place on September 18, and the last on September 26. Over the course of 9 days, 11 flights were conducted, with some days featuring more than one flight. An overview of all successful flights is



Sensor model	Name	Manufacturer	Quantity	Acquisition rate [Hz]	Nominal accuracy
BNO 055	BNO1 & BNO2	Bosch	Temperature, acceleration, linear acceleration, angular rate, magnetic field, gravity acceleration, platform orientation	15.3	±1°C (temperature), ±2.5 deg at 25°C (magnetometer)
BMP390	BMP	Bosch	Temperature, absolute pressure	15.3	±0.5°C at 25°C, ±0.5 hPa within 300-1100 hPa, at 25°C
TMP117	TMP	Texas Instruments	Temperature	15.3	±0.1°C across the range of -20°C to +50°C
SHT40	SHT	Sensirion	Temperature and relative humidity (Heater off)	15.3	±0.2°C in the range 0–60°C, ±1.8% RH typical in the range 25–75% RH
SHT31D	SHT3	Sensirion	Temperature and relative humidity (Heater on)	1	±0.3°C in the range 0–90°C, ±2% RH typical in the range 20–80% RH
BME688	BME	Bosch	Temperature, relative humidity, absolute pressure, trace gases	1	±0.5°C typically at 25°C, ±0.6 hPa between 900-1100 hPa at 25°C, ±3% RH between 20% - 80% RH at 25°C
OPC-N3 (SPI)	OPC	Alphasense	Mass concentration of PM10, PM1, and PM2.5 ambient aerosol particles in air, and relative humidity	1	
U-Blox ZED-F9P	GPS	U-Blox	Altitude, latitude, longitude ^a	1	Horizontal position accuracy < 0.06 m, Vertical position accuracy < 0.12 m
PSC 5	SVM	SVM tec	Three-component velocity from five-channel pitot tube	100	±0.018 m/s (±0.25% of Full Scale Span (FSS), with 125 Pa of FSS)

Table 1. Instrumentation of the WinDart.

^aCheck manual for the entire list of quantities.

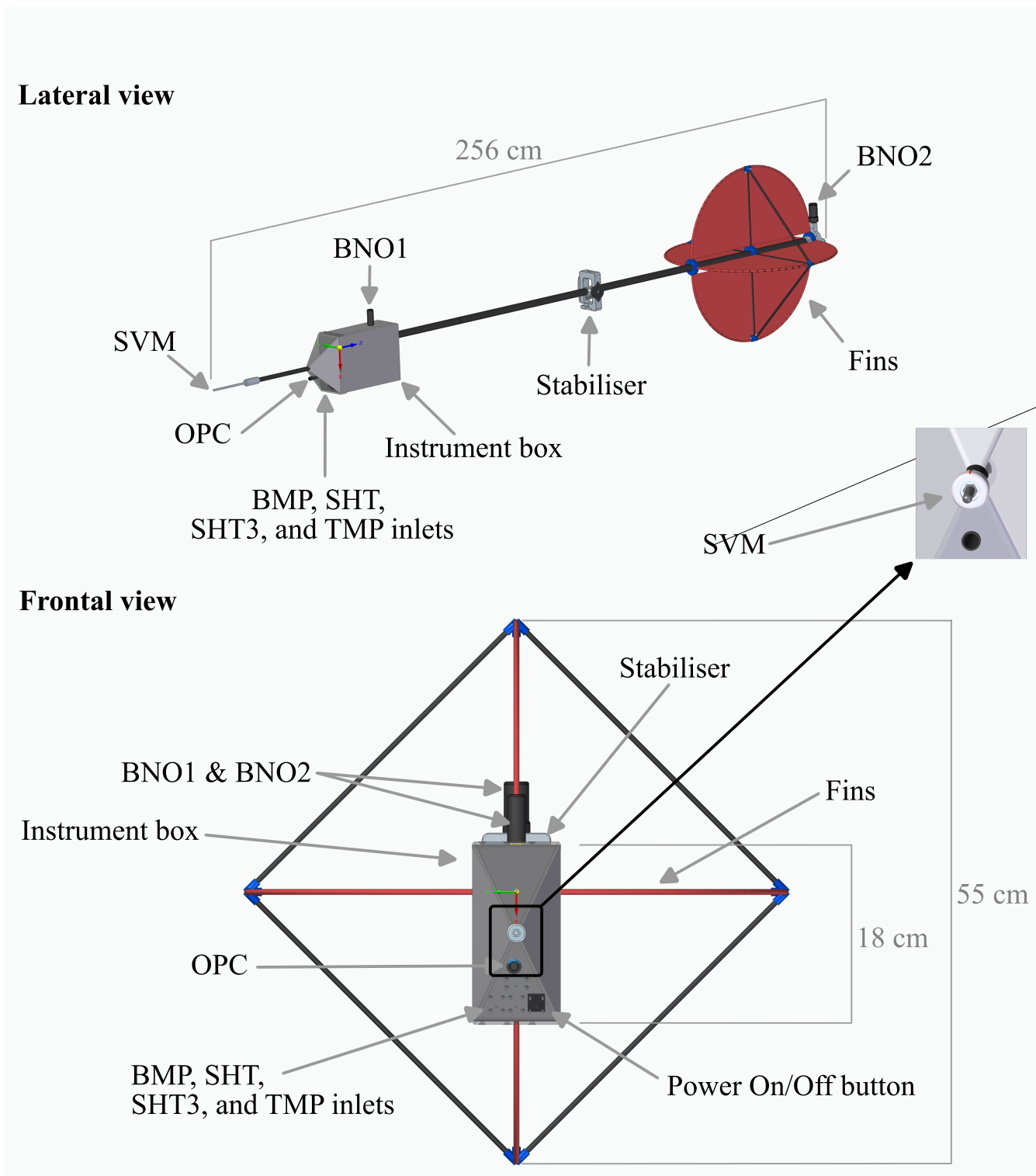


Figure 4. Lateral and frontal views of the WinDart, showing its main scientific instruments, body structure, including fins and stabiliser.



115 presented in table 2. In most flights except for flight 20220925.1335, the WinDart identified as WD1-2 was tethered above the WinDart labelled WD1-1, resulting in WD1-2 taking off first and landing last. The total duration of deployment across all flights amounted to almost 3 days and 10 hours, 38 minutes, 10 seconds.

The naming convention is **DS.MPWD.b1.yyyymmdd.hhmm.nc**, where:

- **DS** is the institute identifier (Dynamics and Self-Organization).
- 120 – **MPWD** is the instrument identifier (Max Planck WinDarts).
- **b1** indicates the data file processing level, with quality control (QC) checks applied; missing data points or those with bad values are set to -9999.9.
- **yyymmdd.hhmm** is the flight ID
- **yyymmdd** denotes the file date (UTC) in year, month, day format.
- 125 – **hhmm** represents the file start time (UTC) in hours and minutes format.

3.3 Ground weather station

A ground-based weather station was deployed to provide complementary meteorological and atmospheric measurements, offering near-surface context for the WinDarts measurements at altitude and enhancing the overall vertical characterisation of the atmospheric environment, as well as for determining safe operating conditions for the MPCK platform by monitoring airspace and lightning risk. The station, with location shown in figure 1, had multiple sensors to monitor wind conditions, atmospheric properties, airspace activity, and electrical discharges, see figure 3.

Wind measurements were obtained from two independent sensors: a Metek uSonic3 Class A-MP ultrasonic anemometer, which provided 3D wind velocity measurements at 30 Hz with a minimum detectable wind speed of 0.1 m/s, and a Lufft WS500UMB weather station, which included a 2D wind sensor along with pressure, temperature, and humidity sensors. High-frequency humidity and trace gas concentrations were measured using a Li-Cor LI-7500DS, a fast-response infrared gas analyzer designed for eddy covariance applications. Additionally, airspace monitoring was performed using a pingStation (uAvionix), which detected aircraft equipped with Mode S or ADS-B transponders. To assess atmospheric electricity, the station included a Campbell Scientific CS110 electric field meter for measuring the local electric field and a Boltek LD-250 lightning detector to track lightning activity in the vicinity.

140 The ground weather station recorded meteorological parameters continuously from the 13th until the 28th of September.

Data availability. All files are archived under individual DOIs at the Zenodo Open Science data archive (zenodo.org) where a dedicated community, Pallas Cloud Experiment – PaCE2022, has been established. This community hosts the data files along with additional metadata related to the data sets. Code for data processing is available from the corresponding author upon reasonable request.



Flight ID	Notes from campaign logbook	ID	Start of recording time (UTC)	Take off time (UTC)	Landing time (UTC)	End of recording time (UTC)	Total duration of flight	Data available	Max. altitude [m]
20220920.0750	9:03 UTC, WD1-1 entered a cloud	WD1-1	07:24:10	07:50	13:15	14:08:07	6h 43m	GPS, MetQuant, SVM	870
		WD1-2	07:41:36	08:05	13:10	14:07:06	6h 25m	GPS, MetQuant, SVM	530
20220921.0716	features a staircase -altitude profile	WD1-1	06:19:14	07:16	13:32	10:18:14	3h 57m	GPS, MetQuant, SVM	1250
		WD1-2	07:45:29	07:55	13:29	11:18:02	3h 32m	MetQuant, SVM	645
20220922.0908	8:20 UTC, WD1-1 entered cloud	WD1-1	08:38:23	09:08	15:31	15:36:12	6h 57m	GPS, MetQuant, SVM	1360
		WD1-2	09:11:05	09:22	15:23	15:35:21	6h 24m	MetQuant, SVM	1135
20220923.0620	8:20 UTC, WD1-1 entered cloud	WD1-1	06:11:21	06:20	08:56	09:03:21	2h 51m	GPS, MetQuant, SVM	700
		WD1-2	06:31:36	07:18	08:37	09:05:06	2h 33m	MetQuant, SVM	190
20220923.1237	Helikites remained above it	WD1-1	12:30:03	12:37	15:29	15:38:29	3h 8m	GPS, MetQuant, SVM	905
		WD1-2	12:43:48	12:52	15:23	15:37:24	2h 53m	MetQuant, SVM	735
20220924.0735	9:28 UTC wind shear observed in one WD, with light rain and broken stratocumulus lenticularis	WD1-1	07:25:46	07:35	13:52	13:57:41	6h 31m	GPS, MetQuant, SVM	1510
		WD1-2	07:26:40	08:15	13:10	13:12:54	5h 46m	MetQuant, SVM	705
20220925.0603	WD1-2 failed to record data due to unknown issues	WD1-1	05:56:50	06:03	11:21	11:25:29	5h 28m	GPS, MetQuant, SVM	1075
		WD1-1	13:31:40	13:35	14:29	14:31:42	1h	GPS, MetQuant, SVM	660
20220925.1335	inter-comparison flight, WDs separated by only 3 m along the main tether	WD1-1	13:27:10	13:35	14:29	14:33:23	1h 6m	MetQuant, SVM	663
		WD1-2	05:00:39	05:30	08:51	10:46:11	5h 45m	GPS(failed), MetQuant, SVM	1245
20220926.0530	WD1-1 penetrated a thin cloud layer at 6:11 UTC and passed through another at 6:21 UTC	WD1-1	05:04:39	06:19	08:43	10:47:17	5h 42m	MetQuant, SVM	930
		WD1-2	11:22:13	11:28	14:09	14:21:13	2h 58m	GPS(failed), MetQuant, SVM	890
20220926.1128	light drizzle was recorded	WD1-1	11:31:22	11:39	14:15	14:19:51	2h 48m	MetQuant, SVM	510
		WD1-2	11:31:22	11:39	14:15	14:19:51	2h 48m	MetQuant, SVM	510

Table 2. Overview of flights for the two WinDarts during the PaCE field campaign. The times for take-off and landing are based on recorded altitude. In the data availability column, "MetQuant" indicates that all devices listed in table 1 measuring meteorological quantities were operational: BMP, TMP, SHT, SHT3, BME, OPC and also BNO1 and BNO2. SVM is the nomenclature given to the PSC5 pitot tube. Logbook notes are recorded on site and may differ slightly from the actual data recorded, but are included for the sake of completeness.



The data are provided in both ASCII comma-separated value (CSV) format
145 – <https://doi.org/10.5281/zenodo.14858142> (Chávez-Medina et al., 2025a)

and Network Common Data Form (NetCDF) format

– <https://doi.org/10.5281/zenodo.14774327> (Chávez-Medina et al., 2025b)

following a standardised file naming convention described in subsection 3.2.1: “**DS.XXXX.b1.yyyymmdd.hhmm.nc/csv**.” Here, **.nc** and
150 **.csv** denote the NetCDF and CSV file formats, respectively, while XXXX represents the instrument identifier: **MPWD** for Max Planck
WinDarts and **GDST** for the ground weather station.

Ahead, in Section 5, we will provide a complete description of the file structure, detailing how the data is organised within
the NetCDF and CSV formats.

4 Data Description

In this section, we present an explanation of the data, using WD1-1 and flight 20220920.0750 as an example as it includes one
155 of the most complete measurements.

4.1 Level 1 data: quality control and data synchronisation

In this context, “Level 1 data” refers to the raw, minimally processed data, i.e. the parsing of data, synchronisation between
different sensor time stamps, the filling of missing values and the generation of validity identifiers. Each flight’s data and
instruments underwent quality control and were standardised into a common format for subsequent release and analysis. This
160 format adheres to the Climate and Forecast (CF) convention for units and nomenclature. Detailed specifications and guidelines
for the CF convention can be found in the official documentation at <http://cfconventions.org/>. For each flight and WinDart, we
created a NetCDF file, as indicated in table 2. All times in this manuscript are presented in UTC. During September, Finland
observes Eastern European Summer Time (EEST), which is UTC+3 hours, meaning local time was 3 hours ahead of UTC
during the campaign.

165 Instruments were calibrated prior to the campaign. The acquired data sets were reviewed to eliminate defective measurements
from further analysis. Defective data were identified graphically. We plotted a set of quantities for each flight and different
devices to verify that the instruments functioned properly throughout the flight and that the measurements were coherent.
Systematic errors were identified thanks to the redundant measurement design of the WinDarts. As shown in table 1, different
instruments measured the same quantity, allowing for cross-verification. For instance, we compared GPS-measured altitude
170 with altitude derived from barometric pressure measured by the BMP.

Defective measurements are not included in table 2. In cases where a device malfunctioned at some point after the beginning
of the flight, we documented the failure in the metadata of the corresponding NetCDF file and indicated it in table 2 by labeling
it as “(failure)” or excluding it from data availability. Figure 5 illustrates two flights with failures. The upper plot depicts
flight 20220921.0716, where both WinDarts experienced battery failures mid-flight, resulting in the simultaneous failure of all

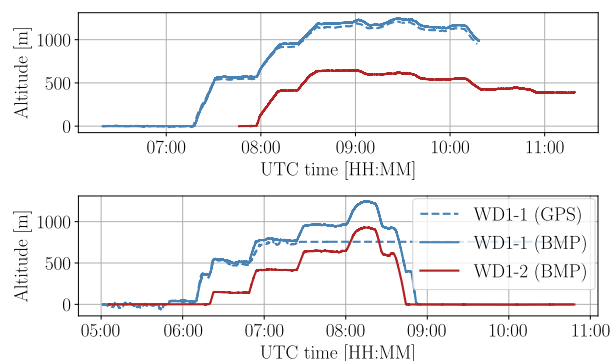


Figure 5. Altitude profiles for flight 20220921.0716 (top) and flight 20220926.0530 (bottom) are presented here. Top plot is an example of complete device failure during a flight. Bottom plot is an example of GPS device failure during a flight. The dashed line represents measurements obtained from the GPS, while the solid line indicates altitude calculated using barometric pressure data from the BMP. Time is displayed in UTC, with local time being UTC+3 hours.

175 instruments on each WinDart. For WD1-1 the failure occurred at 10:18 UTC and for WD1-2 at 11:18 UTC. The lower plot
shows flight 20220926.0530, where the GPS on WD1-1 failed during the flight. This case exemplifies how the redundancy
of the WinDarts aided in error detection. The label BMP indicates that altitude was computed from the barometric pressure
measured by the BMP. Notably, the GPS on WD1-2 failed at the start of both flights.

Level 1 data processing also involves synchronising all measurements and correcting timestamps. We used the UTC times-
180 tamps from the GPS as the authoritative reference, which can be accurate to microseconds. Consequently, all measurements
(SVM, BPM, TMP, SHT, etc.) were aligned to the GPS timestamps.

As shown in table 2, while the GPS data was not always completely reliable, at least one of the WinDarts maintained
functional GPS throughout all flights except 20220926.0530 and 20220926.1128, which are marked as “GPS(failed)” in the
table. In these cases, although the GPS did not record continuous data, it successfully captured the start time of the flight,
185 allowing for reasonably accurate synchronisation of other measurements.

In flight 20220920.0750, when both WinDarts’ GPS systems were operational, synchronisation was most precise, achieving
microsecond accuracy. Each WinDart’s data was aligned to its respective GPS timestamps. However, in cases where one GPS
failed (typically WD1-2’s), we synchronised its measurements to WD1-1’s GPS timestamps by aligning altitude patterns.
Specifically, we compared the altitude derived from WD1-2’s pressure sensor (BMP) to the altitude recorded by WD1-1’s
190 GPS. This manual synchronisation process allowed us to establish a reliable UTC timestamp for WD1-2’s data.

Figure 6 presents the time series of air temperature, pressure, relative humidity, and altitude recorded by each sensor on
WinDart WD1-1 during flight 20220920.0750. In each plot, the primary sensor for each quantity—selected based on the
highest accuracy and resolution specified in the manufacturers’ manuals (see table 1)—is highlighted with a thicker line: TMP
for temperature, BMP for pressure, and SHT (heater off) for relative humidity.

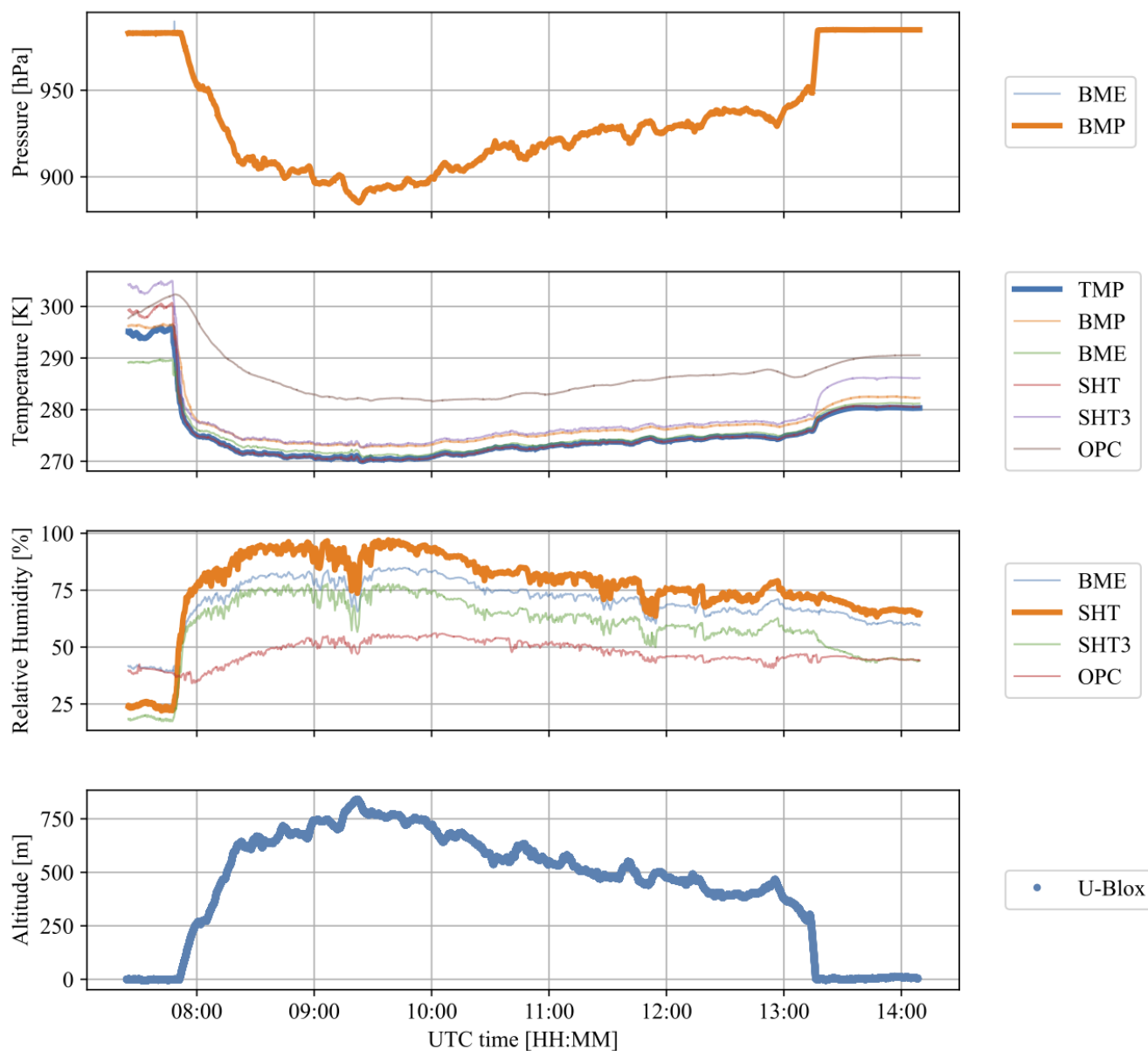


Figure 6. Time series of air pressure , air temperature , relative humidity and altitude for WD1-1 during flight 20220920.0750 of the PaCE campaign. Local time is UTC+3 hours.

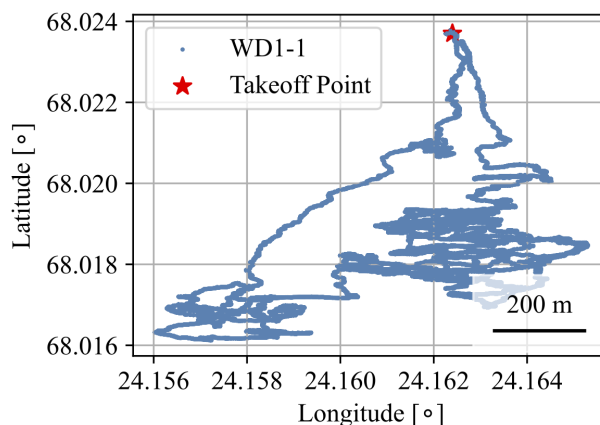


Figure 7. Location of WD1-1 during flight 20220920.0750.

195 Figure 7 displays the longitude and latitude coordinates of WD1-1 throughout flight 20220920.0750. This spatial representation shows the flight path taken during the data collection. The plotted trajectory highlights how WD1-1's position changed over time, allowing for a clear visualization of the flight's movement.

During some flights, the WinDarts entered clouds, as initially determined by visual inspection during flight (which is not highly accurate) and later verified by particle concentration measurements. Figure 8 presents a scatter plot of particle concentration from the OPC on WD1-1 across different size bins during flight 20220920.0750. Each point represents a concentration measurement, with a colour gradient indicating particle size from the smallest to the largest bins.

200 According to the flight log, WD1-1 entered a cloud around 09:03. However, figure 8 suggests an earlier entry, as a noticeable increase in particle concentration across all size bins is observed around 08:30. This highlights the impact of cloud droplets on particle distribution within the measured range.

205 Figure 9 illustrates the time series of the air velocity vector in the platform (WinDart) frame, denoted as $\mathbf{U} = (U, V, W)$, as measured by the SVM (five-pressure-channel Pitot tube). The Pitot tube measures five differential pressures, which are then processed using Vectoflow Post-Processing libraries to obtain the wind velocity vector \mathbf{U} . The Vectoflow function used the air temperature and air pressure time series recorded by the TMP and BMP sensors, respectively (refer to figure 6). At this stage, no additional post-processing techniques are applied to the velocity measurements. The components (U, V, W) represent the wind-direction, transversal-to-wind-direction, and vertical-direction components of \mathbf{U} . Due to the fins installed in their tails (illustrated in figure 4), the WinDarts align with the wind direction.

215 Figure 10 shows the time series of air temperature, wind speed, relative humidity, and atmospheric vertical electric field recorded by the ground weather station during the 20th of September, when the WinDarts performed flight 20220920.0750. For each quantity, the primary sensor was chosen as the one offering the highest accuracy and resolution according to the specifications provided in the manufacturers' manuals: the Luftt WS500UMB for temperature and relative humidity, the Metek uSonic3 Class A-MP for wind speed, and the Campbell Scientific CS110 field mill for the electric field.

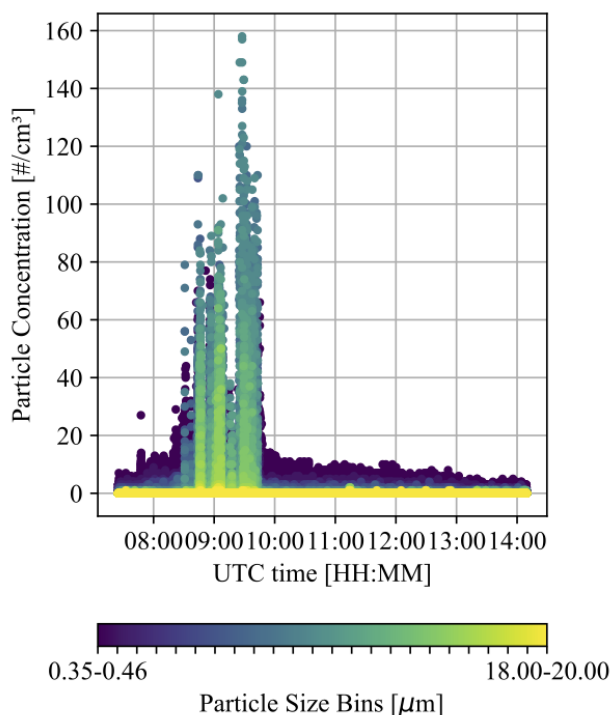


Figure 8. Time series plot showing particle concentration measured by an Alphasense OPC-N3 optical particle counter during flight 20220920.0750. Each curve represents a specific particle size bin, with bins spanning from 0.35 to 20 μm in diameter: Bin 0 (0.35-0.46 μm), Bin 1 (0.46-0.66 μm), Bin 2 (0.66-0.77 μm), Bin 3 (0.77-0.96 μm), Bin 4 (0.96-1.15 μm), Bin 5 (1.15-1.34 μm), Bin 6 (1.34-1.52 μm), Bin 7 (1.52-1.75 μm), Bin 8 (1.75-2.00 μm), Bin 9 (2.00-2.35 μm), Bin 10 (2.35-2.71 μm), Bin 11 (2.71-3.24 μm), Bin 12 (3.24-3.80 μm), Bin 13 (3.80-4.40 μm), Bin 14 (4.40-5.20 μm), Bin 15 (5.20-6.00 μm), Bin 16 (6.00-7.00 μm), Bin 17 (7.00-8.00 μm), Bin 18 (8.00-10.00 μm), Bin 19 (10.00-12.00 μm), Bin 20 (12.00-14.00 μm), Bin 21 (14.00-16.00 μm), Bin 22 (16.00-18.00 μm), Bin 23 (18.00-20.00 μm). Concentrations are shown over time.

5 File Structure

The data are provided in both ASCII comma-separated values (CSV) and Network Common Data Form (NetCDF).

5.1 NetCDF

220 The NetCDF contains a hierarchical structure that organises data based on instrument type and measurement platform. Each file begins at the root level, containing the filename as the top-level group. All groups and variables are accompanied by detailed metadata (i.e. attributes), including units, descriptions, and sensor specifications.

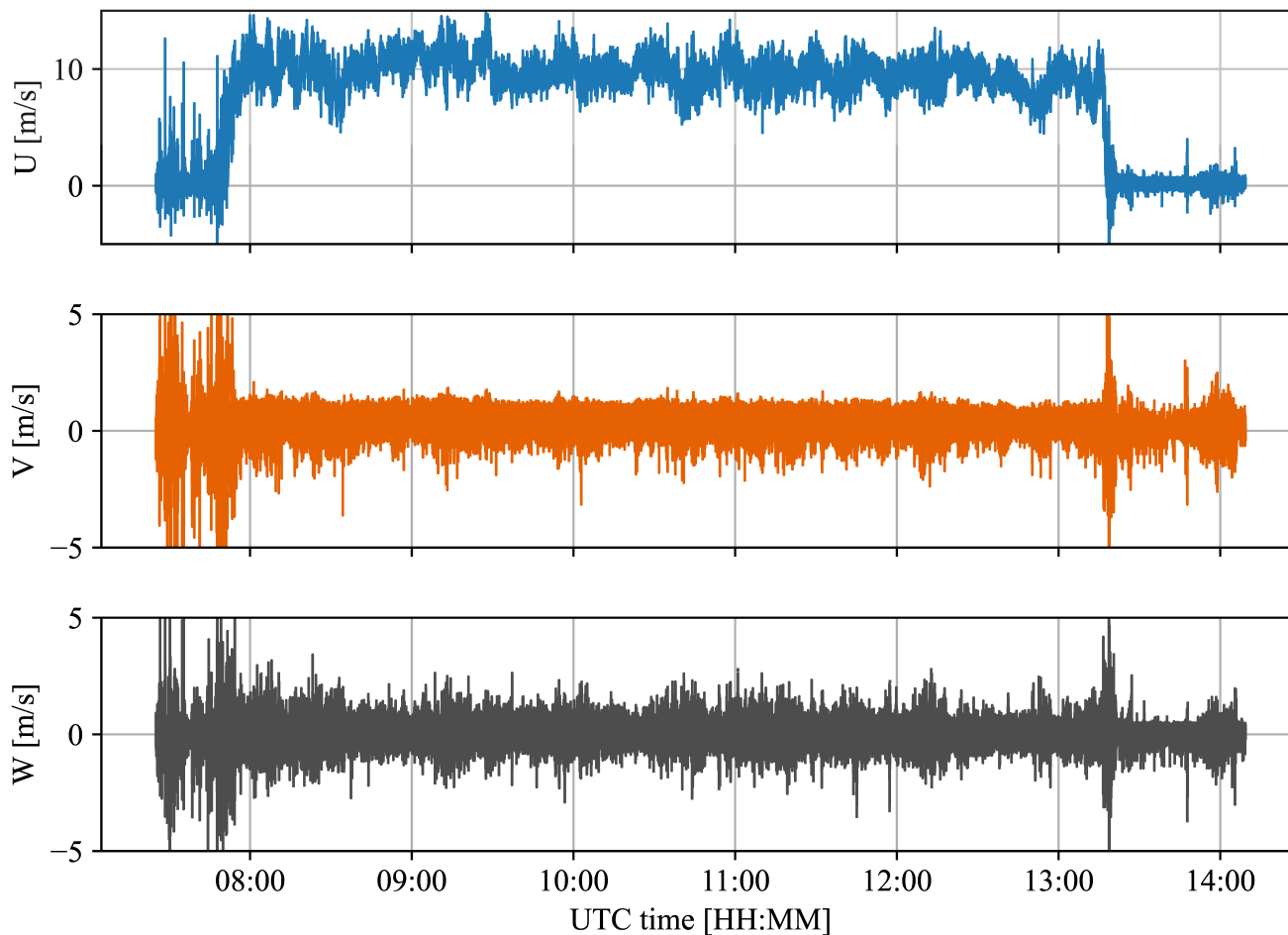


Figure 9. The time series of the wind velocity vector measured by WinDart WD1-1 during flight 20220920.0750 of the PaCE campaign is presented here. The time series corresponds to the wind velocity vector as measured by the platform, without any corrections for platform motion. All times are displayed in UTC, with local time being UTC+3 hours.

5.1.1 WinDarts

At the first level of the hierarchy, the data set is grouped under “Level1”, which contains data from individual WinDart platforms, specifically WD1-1 and WD1-2, each corresponding to an independent measurement system.

Each WD1 subgroup is further divided into three main categories based on the source of measurement:

- arduino (referred to as MetQuant in table 2): This group contains measurements from sensors connected to an Arduino-based system, including:
 - BME: Air pressure, temperature, and relative humidity.

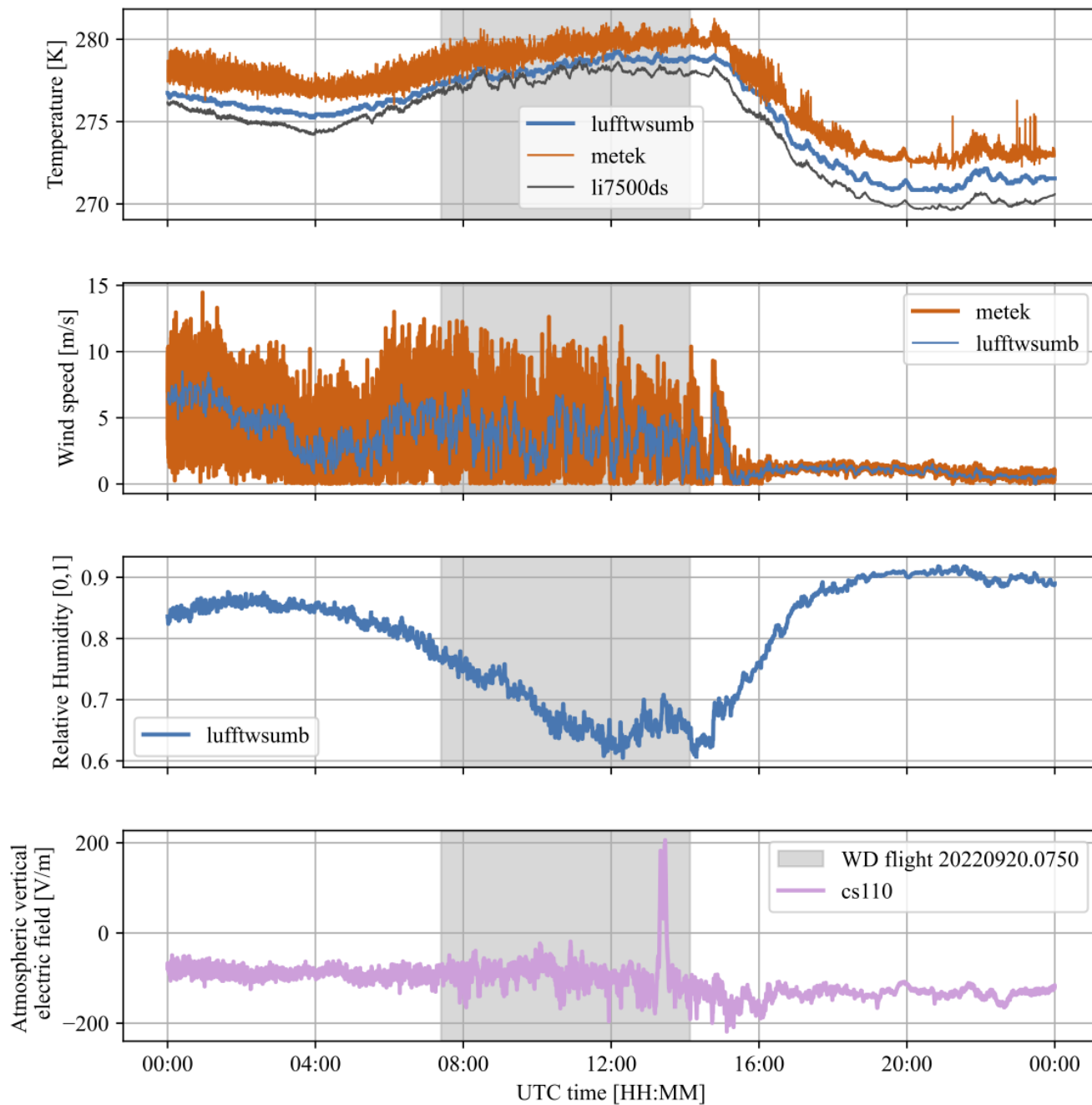


Figure 10. Time series of air temperature, wind speed, relative humidity and atmospheric vertical electric field measured by the ground weather station during the 20.09.2022. Local time is UTC+3 hours. The period of time during which the WinDarts were flying (20220920.0750) is indicated by the grey box.



- 230
- BMP: Additional pressure measurements.
 - BNO1, BNO2: Inertial measurement unit (IMU) data.
 - OPC: Optical particle counter data.
 - SHT, SHT3: Additional temperature and humidity measurements.
 - TMP: High-precision temperature sensor.
- 235
- gps: This group includes position, velocity, and time synchronization information from the GPS unit, such as altitude, latitude, longitude, horizontal and vertical accuracy, geoidal height, magnetic declination, and timestamps.
 - svm: This group contains Mach number, Reynolds number, static and dynamic pressure, velocity components, and total temperature.

At the lowest level of the hierarchy, each sensor-specific group (e.g., BME, BMP, GPS, SVM) contains the measured variables along with their associated time arrays.

240

5.1.2 Ground weather station

The data set is also organised into different groups and subgroups that correspond to specific instruments and measurement categories. At the first level of the hierarchy, the data set is grouped under “Level1”, which contains multiple subgroups corresponding to different sensor systems:

- 245
- boltek250: This is the lightning strike detector, which measures range and direction of strikes.
 - cs110: Contains the raw and calculated electric field.
 - li7500ds: Optical H₂O and CO₂ analyser with meteorological quantities such as air temperature and air pressure.
 - lightning_warning_gnss: This group contains GPS-based positioning data related to the position of the boltek250.
 - lufftsumb: Contains readings from a weather station module.
- 250
- metek: Includes high-resolution atmospheric data including wind velocity and temperature measurements.
 - pingstation: Stores satellite-based positioning data for airspace monitoring.
 - tensiometer: Contains the line tension to the balloon.

At the lowest level of the hierarchy, each sensor-specific group contains the measured variables along with their corresponding time arrays.



255 5.2 CSV

The CSV files are organised in a structured format that mirrors the hierarchical nature of the NetCDF format. Each file contains two main columns:

- Path – This column specifies the location of each variable within the data set using a structured naming convention. The path follows a hierarchy, separating different levels with slashes (/). For example, for the WinDarts:

260 /Level1/WD1-1/arduino/BNO1/time
 /Level1/WD1-1/arduino/BNO1/acceleration
 /Level1/WD1-1/arduino/BNO2/magnetic_field

This structure reflects the source of the data, the specific sensor (e.g., BNO1 or BNO2), and the type of measurement recorded.

- 265 – Data – This column contains the recorded values associated with each path. The values are stored as lists or arrays, maintaining the sequential nature of the measurements. For instance, the time variable consists of an array of timestamps, while acceleration or magnetic_field variables contain numerical arrays corresponding to their respective sensor readings.

This format ensures that the CSV files retain the same level of organization and clarity as the original data set, allowing users to easily locate and interpret specific variables. The structured naming convention makes it intuitive to analyze data relationships
270 across different sensors and measurement types.

6 Possible end users

This data set is designed for researchers investigating the atmospheric boundary layer, offering high-resolution measurements of meteorological variables that facilitate the characterisation of vertical profiles and fluxes within the surface layer, mixed layer, and entrainment zone. For an analysis of long-term trends, we recommend performing a diurnal cycle assessment.

275 The data set includes example cases of convective boundary layers, such as flight 20220920.0750 (see Chávez Medina (2024)), and serves as an input for model development, a reference for instrument validation, and a resource for synergistic analyses with complementary PaCE campaign measurements, including remote sensing data, UAV observations, and cloud microphysics. The data collected from the MPCK platform and associated instruments is particularly useful for atmospheric scientists studying turbulence in the boundary layer and cloud-turbulence interactions.

280 To gain a full understanding of boundary layer dynamics and thermodynamics, we recommend integrating this data set with the MPCK+ data set (Schlenczek et al., 2025) and FishBox measurements both part of this special issue.

For an example application of statistical analysis in a convective boundary layer, refer to Chapters 5 and 6 of Chávez Medina (2024).



285 *Author contributions.* HK, and GB designed, and assembled the WinDarts. GB and HK wrote the control software. FN, OS, CB, and EB performed in-situ measurements and collected the data. VCM, FN and GB wrote the parsing codes. VCM post-processed and prepared the data, and wrote the first draft of this manuscript. All authors contributed to writing the final version of the manuscript.

Competing interests. The authors declare no competing interests. The sponsors had no influence on the study design, data collection and analysis, decision to publish, or preparation of the manuscript.

290 *Acknowledgements.* We would like to thank David Brus from the Finnish Meteorological Institute for making it possible for us to take part in the campaign and for his active support during our field work. We thank Michael Wilczek for his input during the preparation of the campaign. We also acknowledge Constantin Schettler and Marcel Meyer for their contributions to in-situ measurements and data collection. Thanks go to Andreas Kopp and Dr. Artur Kubitzek for organizing the campaign logistics. The development and manufacturing of mechanical components and electronics were carried out in collaboration with the in-house machine shop and scientific electronics team. The development of the MPCK platform and the WinDarts was funded by internal funds of the Max Planck Society.



295 References

- Brus, D., Douglgeris, K., Bagheri, G., Bodenschatz, E., Chavez-Medina, V., Schlenczek, O., Khodamoradi, H., Pohorsky, R., Schmale, J., Lonardi, M., Favre, L., Böhmländer, A., Möhler, O., Lacher, L., Girdwood, J., Gratzl, J., Grothe, H., Kaikkonen, V., Molkoselkä, E., Mäkynen, A., O'Connor, E., Leskinen, N., Tukainen, S., Le, V., Backman, J., Luoma, K., Servomaa, H., and Asmi, E.: Data generated during the Pallas Cloud Experiment 2022 campaign: An introduction and overview, *Earth System Science Data*, 2025.
- 300 Chávez Medina, V.: Turbulence in convective boundary layers: a statistical investigation, Ph.D. thesis, Georg-August University School of Science, 2024.
- Chávez-Medina, V., Bagheri, G., and Bodenschatz, E.: Data from the Max Planck WinDarts and Ground Weather Station during the Pallas Cloud Experiment 2022, <https://doi.org/10.5281/zenodo.14858143>, 2025a.
- Chávez-Medina, V., Bagheri, G., and Bodenschatz, E.: Data from the Max Planck WinDarts and Ground Weather Station during the Pallas
305 Cloud Experiment 2022, <https://doi.org/10.5281/zenodo.14774328>, 2025b.
- Douglgeris, K. M., Lihavainen, H., Hyvärinen, A.-P., Kerminen, V.-M., and Brus, D.: An extensive data set for in situ microphysical characterization of low-level clouds in a Finnish sub-Arctic site, *Earth System Science Data*, 14, 637–649, <https://doi.org/10.5194/essd-14-637-2022>, 2022.
- Gratzl, J., Brus, D., Douglgeris, K., Böhmländer, A., Möhler, O., and Grothe, H.: Fluorescent aerosol particles in the Finnish sub-Arctic during
310 the Pallas Cloud Experiment 2022 campaign, *Earth System Science Data Discussions*, 2025, 1–20, <https://doi.org/10.5194/essd-2024-543>, 2025.
- Schlenczek, O., Nordsiek, F., Brunner, C., Chavez-Medina, V., Thiede, B., Bodenschatz, E., and Bagheri, G.: Airborne measurements of turbulence and cloud microphysics during PaCE 2022 using the Advanced Max Planck CloudKite Instrument (MPCK⁺), *Earth System Science Data*, 2025.
- 315 Schröder, M.: Cloud Microphysics Investigations with the Cloudkite Laboratory, Ph.D. thesis, Georg-August-Universität Göttingen Göttingen, 2023.
- Stevens, B., Bony, S., Farrell, D., Ament, F., Blyth, A., Fairall, C., Karstensen, J., Quinn, P. K., Speich, S., Acquistapace, C., Aemisegger, F., Albright, A. L., Bellenger, H., Bodenschatz, E., Caesar, K.-A., Chewitt-Lucas, R., de Boer, G., Delanoë, J., Denby, L., Ewald, F., Fildier, B., Forde, M., George, G., Gross, S., Hagen, M., Hausold, A., Heywood, K. J., Hirsch, L., Jacob, M., Jansen, F., Kinne, S., Klocke, D.,
320 Kölling, T., Konow, H., Lathon, M., Mohr, W., Naumann, A. K., Nuijens, L., Olivier, L., Pincus, R., Pöhlker, M., Reverdin, G., Roberts, G., Schnitt, S., Schulz, H., Siebesma, A. P., Stephan, C. C., Sullivan, P., Touzé-Peiffer, L., Vial, J., Vogel, R., Zuidema, P., Alexander, N., Alves, L., Arix, S., Asmath, H., Bagheri, G., Baier, K., Bailey, A., Baranowski, D., Baron, A., Barrau, S., Barrett, P. A., Batier, F., Behrendt, A., Bendinger, A., Beucher, F., Bigorre, S., Blades, E., Blossey, P., Bock, O., Böing, S., Bosser, P., Bourras, D., Bouruet-Aubertot, P., Bower, K., Branellec, P., Branger, H., Brennek, M., Brewer, A., Brilouet, P.-E., Brüggemann, B., Buehler, S. A., Burke, E.,
325 Burton, R., Calmer, R., Canonici, J.-C., Carton, X., Cato Jr., G., Charles, J. A., Chazette, P., Chen, Y., Chilinski, M. T., Choulaton, T., Chuang, P., Clarke, S., Coe, H., Cornet, C., Coutris, P., Couvreur, F., Crewell, S., Cronin, T., Cui, Z., Cuypers, Y., Daley, A., Damerell, G. M., Dauhut, T., Deneke, H., Desbios, J.-P., Dörner, S., Donner, S., Douet, V., Drushka, K., Dütsch, M., Ehrlich, A., Emanuel, K., Emmanouilidis, A., Etienne, J.-C., Etienne-Leblanc, S., Faure, G., Feingold, G., Ferrero, L., Fix, A., Flamant, C., Flatau, P. J., Foltz, G. R., Forster, L., Furtuna, I., Gadian, A., Galewsky, J., Gallagher, M., Gallimore, P., Gaston, C., Gentemann, C., Geyskens, N., Giez, A.,
330 Gollop, J., Gouirand, I., Gourbeyre, C., de Graaf, D., de Groot, G. E., Grosz, R., Güttler, J., Gutleben, M., Hall, K., Harris, G., Helfer, K. C., Henze, D., Herbert, C., Holanda, B., Ibanez-Landeta, A., Intrieri, J., Iyer, S., Julien, F., Kalesse, H., Kazil, J., Kellman, A., Kidane,



335 A. T., Kirchner, U., Klingebiel, M., Körner, M., Kremper, L. A., Kretzschmar, J., Krüger, O., Kumala, W., Kurz, A., L'Hégaret, P., Labaste,
M., Lachlan-Cope, T., Laing, A., Landschützer, P., Lang, T., Lange, D., Lange, I., Laplace, C., Lavik, G., Laxenaire, R., Le Bihan, C.,
Leandro, M., Lefevre, N., Lena, M., Lenschow, D., Li, Q., Lloyd, G., Los, S., Losi, N., Lovell, O., Luneau, C., Makuch, P., Malinowski,
S., Manta, G., Marinou, E., Marsden, N., Masson, S., Maury, N., Mayer, B., Mayers-Als, M., Mazel, C., McGeary, W., McWilliams, J. C.,
340 Mech, M., Mehlmann, M., Meroni, A. N., Mieslinger, T., Minikin, A., Minnett, P., Möller, G., Morfa Avalos, Y., Muller, C., Musat, I.,
Napoli, A., Neuberger, A., Noisel, C., Noone, D., Nordsiek, F., Nowak, J. L., Oswald, L., Parker, D. J., Peck, C., Person, R., Philippi, M.,
Plueddemann, A., Pöhlker, C., Pörtge, V., Pöschl, U., Pologne, L., Posyniak, M., Prange, M., Quiñones Meléndez, E., Radtke, J., Ramage,
K., Reimann, J., Renault, L., Reus, K., Reyes, A., Ribbe, J., Ringel, M., Ritschel, M., Rocha, C. B., Rochetin, N., Röttenbacher, J., Rollo,
345 C., Royer, H., Sadoulet, P., Saffin, L., Sandiford, S., Sandu, I., Schäfer, M., Schemann, V., Schirmacher, I., Schlenczek, O., Schmidt, J.,
Schröder, M., Schwarzenboeck, A., Sealy, A., Senff, C. J., Serikov, I., Shohan, S., Siddle, E., Smirnov, A., Späth, F., Spooner, B., Stolla,
M. K., Szkółka, W., de Szoeko, S. P., Tarot, S., Tetoni, E., Thompson, E., Thomson, J., Tomassini, L., Totems, J., Ubele, A. A., Villiger,
L., von Arx, J., Wagner, T., Walther, A., Webber, B., Wendisch, M., Whitehall, S., Wiltshire, A., Wing, A. A., Wirth, M., Wiskandt, J.,
Wolf, K., Worbes, L., Wright, E., Wulfmeyer, V., Young, S., Zhang, C., Zhang, D., Ziemer, F., Zinner, T., and Zöger, M.: EUREC⁴A,
345 Earth System Science Data, 13, 4067–4119, <https://doi.org/10.5194/essd-13-4067-2021>, 2021.